Towards understanding the role of K during biomass steam gasification

Tilia Dahou, Françoise Defoort, Mejdi Jeguirim, Capucine Dupont

Towards understanding the role of K during biomass steam gasification

Tilia DAHOU[a,b,c,d], Françoise DEFOORT[a], Mejdi JEGUIRIM[b,c*], Capucine DUPONT[e]

[a]Université Grenoble Alpes, CEA, LITEN, DTBH, 17 avenue des Martyrs, 38054 Grenoble CEDEX 09, France

[b]Université de Haute-alsace, CNRS, IS2M UMR 7361, 68100 Mulhouse, France

[c]Université de Strasbourg, France

[d]Agence de l'Environnement et de la Maîtrise de l'Energie (ADEME), 20 avenue du Grésillé, BP 90406, 49004 Angers CEDEX 01, France

[e]IHE Delft Institute for Water Education, Westvest 7, 2611 AX Delft, The Netherlands

*Corresponding author: mejdi.jeguirim@uha.fr

Highlights

- Rice husk steam gasification was conducted with K_2CO_3 added without direct contact
- A two-compartment thermobalance crucible was used to assess the gas phase influence
- The K-catalysis mechanisms involve the gas phase, most likely with formed KOH(g)
- Both pyrolysis and steam gasification steps are catalyzed by K
- The K-catalysis competes with the reaction of K with SiO_2 inherent to biomass

Abstract

Steam gasification is known to be catalyzed by K. However, the exact mechanisms are not identified to this day. In the present study, the catalytic influence of K on biomass steam

gasification and its interaction with Si was investigated. The study was conducted through thermogravimetric analysis (TGA) on rice husks as a Si-rich biomass and K_2CO_3 as a model K-compound. Experiments were conducted in three different configurations: biomass or inorganic compound alone; mixtures of biomass and inorganic powders; biomass and inorganic compound without contact in a two-compartment crucible. It was shown that K has a catalytic effect on both the pyrolysis and the gasification steps. These effects occur even when the K-compound is not in direct contact with the biomass. Therefore, it demonstrates that the mechanisms involve the gas phase through the volatilization of a K-compound, most likely KOH(g). However, the observed catalytic effect on rice husks was weaker than the effect obtained in the case of beech wood, a Si-poor and more generally ash-poor biomass, under the same conditions. It shows that there is a competition between i) the influence of K on the biomass pyrolysis and char gasification kinetics and ii) the interaction of K with SiO_2 inherent to the biomass.

Keywords

steam gasification; reaction kinetics; catalysis; potassium; silica; rice husk

1. Introduction

To develop bioenergy production, agricultural residues represent an interesting source as they have an important availability and do not decrease the surface of land available for food production. However, agricultural residues can be problematic during the gasification process due to high inorganic contents compared to woods. Their main inorganic elements are generally Si, K and Ca [1]. Such elements can be detrimental to the gasification process by inducing slag formation and/or agglomeration of the gasifier bed [2,3]. Moreover, they can have a strong effect on the reaction kinetics which may influence the biomass residence time inside the reactor and therefore the gasifier design. In this context, the residence time must be adapted either to reach the highest conversion possible or to purposely have a remaining

47 char that can be burnt in order to bring the required heat to the process, depending on the
48 gasifier technology.

49 Alkali and alkaline earth metals (AAEMs) tend to have a catalytic effect that enhances
50 biomass gasification kinetics. More specifically, alkali metals, and in particular K which is
51 more present in biomass than Na [1], are reported to be more active than alkaline earth
52 metals. The catalytic activity of AAEMs was reported to be, in decreasing order, K, Na, Ca
53 and Mg [4–6]. This ranking has been determined for materials with various ash contents.

54 Catalytic gasification uses this effect to improve the gasification process. Catalysts usually
55 studied are compounds of AAEMs as well as some heavy metal compounds such as Fe-
56 compounds and Ni-compounds [7,8]. In the case of K-catalysis, added compounds are
57 mostly K_2CO_3 and KOH which are compounds naturally found in biomass [7]. KNO_3, KCl or
58 K_2SO_4 have also been studied [9–11]. Authors have found the following relative activity: KOH
59 ~ K_2CO_3 ~ KNO_3 > K_2SO_4 > KCl [12–14]. They have also demonstrated that under steam the
60 intermediate species KOH was formed from all salts [14].

61 Several methods have been used in the literature to highlight the catalytic effects of these
62 inorganic elements. Studies have used raw biomass or biomass char [15–24], biomass or
63 char washed with deionized water and/or with acid to remove the inherent inorganic matter
64 [5,10,20,25–28], or biomass or char with added inorganic compounds [6,9–12,20,26,27,29–
65 37]. These latter ones were prepared through solid mixing [26,29,30,35,37] or impregnated
66 with a solution containing the inorganic compound [6,9–12,27,30–37]. Impregnation has
67 been the major addition method used in literature since it is simple to carry out and allows a
68 close contact between the inorganics and the biomass.

69 Few authors have compared the effects of various addition methods. Elliott *et al.* [37] and
70 Bach-Oller *et al.* [30] have observed a slightly stronger catalytic effect of K_2CO_3 in the case of
71 impregnation compared to dry mixing. Authors have supposed an activity through the gas
72 phase and attributed the slight decrease in activity with dry mixing to a lower inorganic

compound volatilization due to mass transfer limitations. However, to our knowledge, no available investigations have been conducted to identify the gas phase effect of K-catalysts. In addition, several studies in the literature have examined the catalytic CO_2 gasification of biomass species having a low inorganic content [9-12, 25, 31, 33, 35-37].

In this context, the present work aims to contribute to the understanding of the K influence on biomass steam gasification in the case of a Si-rich biomass, in order to better understand the K behavior, its effect through the gas phase and its potential interaction with the inherent SiO_2 of the biomass.

2. Materials and Methods

2.1. Materials

The selected biomass for this study was rice husks (RH) from Camargue, France, a Si-rich biomass. Its behavior was compared to sunflower seed shells (SSS) from Bordeaux, France, a Si-poor and K-rich biomass, and beech wood (BW) from France, Si-poor and more generally ash-poor biomass. The samples were ground below 200 µm in a Pulverisette 14 rotor mill (FRITSCH, Idar-Oberstein, Germany). The ash content and inorganic element composition of the samples were measured according to solid fuel standards NF EN 14775 [38] and NF EN ISO 16967 [39], respectively. The properties of each biomass are summarized in **Table 1**.

Table 1. Composition of rice husks and beech wood (in dry basis).

Property	Unit	Rice husks (RH)	RH + 7wt% K_2CO_3	Sunflower seed shells (SSS)	Beech wood (BW)
Ash at 550 °C	wt%	14.6	20.3**	3.3	0.6
C	wt%	41.6	39.0	50.2	45.9
H	wt%	5.2	4.7	6.5	6.2
O*	wt%	45.1	35.6	40.6	47.1
N	wt%	0.5	0.50	0.7	0.3

S	wt%	0.1	0.09	0.1	0.058
Cl	wt%	0.1	0.09	0.1	0.005
Si	$mg.kg^{-1}$	63955	59518	194	115
K	$mg.kg^{-1}$	5822	44632	9729	910
Ca	$mg.kg^{-1}$	1797	1672	4489	2516
Mg	$mg.kg^{-1}$	659	613	1838	475
P	$mg.kg^{-1}$	981	913	896	75
Na	$mg.kg^{-1}$	413	384	9	3.6
Al	$mg.kg^{-1}$	228	212	150	12
Fe	$mg.kg^{-1}$	192	179	1099	34
Main inorganic elements	—	Si – K – Ca	Si – K – Ca	K – Ca –Mg	Ca – K – Mg

*Total oxygen calculated by difference with all other elements.
**Theoretical, calculated as: $\%K_2CO_3$ + (100 - $\%K_2CO_3$) × Ash of rice husks

A model K-compound was selected for the study: potassium carbonate (K_2CO_3). It was selected since it can be found naturally in biomass [40]. Merck K_2CO_3 EMSURE® ACS, ISO, Reag. Ph. Eur, ≥ 99.0 % was used. The K_2CO_3 powder was ground from around 500 µm to <100 µm with a mortar and pestle, in a N_2 atmosphere to prevent its hydration. It was then kept in a vacuum desiccator.

2.2. Experimental installation and procedure

The steam gasification behavior of the samples was investigated through thermogravimetric analysis (TGA). Experiments were carried out at atmospheric pressure using a Setsys thermobalance (SETARAM, Caluire, France) coupled with a Wetsys steam generator described elsewhere [16].

A home-made crucible was designed for this present investigation. It is a crucible consisting of a cylindrical platinum crucible of 2 mm height and 10 mm diameter with a partition of the same height along its diameter made up of platinum with 5% gold (**Figure 1**). The feed gas is injected from below the crucible.

Figure 1. Divided crucible (here containing RH and K_2CO_3).

Experiments were conducted in three different configurations: biomass or inorganic compound alone; mixtures of biomass and inorganic powders; biomass and inorganic compound without direct contact in the crucible.

Inorganic concentrations were expressed as a percentage of the total sample:

$$\%Inorganic = \frac{m_{Inorganic}}{m_{Inorganic} + m_{Biomass}} \quad (1)$$

With $m_{Inorganic}$ the mass of inorganic added and $m_{Biomass}$ the mass of biomass.

Mixtures of biomass and inorganic powders were prepared with approximately 140 mg of biomass and the necessary mass of inorganic compound to obtain the desired concentration. The two powders were added to a plastic flask with a few glass beads of 3 mm diameter. Homogeneous mixing was obtained by shaking the flask by hand for around one minute.

The TGA sample mass was determined through preliminary experiments on pure biomass to be in the chemical regime in this configuration.

Approximately 15 mg of sample were heated at 24 °C.min^{-1} until 450 °C under 0.05 L.min^{-1} N_2 and kept for 60 min at this temperature. They were then heated at 24 °C.min^{-1} until 800 °C and kept at this temperature until the end of the experiment. Samples were swept by N_2 after the final temperature was reached to ensure pyrolysis completion and mass stability (12 min). Gas was then switched to a mixture of 20 vol% H_2O in N_2 with the same gas flow of

125 0.05 L.min^{-1}. This marked the beginning of the gasification step. The experiment was
126 completed when the mass was stabilized, i.e. when gasification was finished and only ashes
127 remained.

128 Experiments were conducted at least in duplicates to verify repeatability. Only one of the
129 repetitions is plotted.

130 Results were plotted as the normalized mass:

$$\frac{m(t)}{m_i}, \tag{2}$$

131 where m_i and $m(t)$ are the mass of initial raw biomass and the mass measured at the time t,
132 respectively.

133 Gasification solid conversion was defined from the mass loss measured as a function of time
134 during TGA by using the following expression:

$$X(t) = \frac{m_{ichar} - m(t)}{m_{ichar} - m_f}, \tag{3}$$

135 where m_{ichar} and m_f are the mass of char before gasification (at the time of steam injection)
136 and the mass measured at the end of gasification (remaining ash), respectively.

137 The gasification rate was then defined as the variation of conversion versus time:

$$r(t) = \frac{dX}{dt}. \tag{4}$$

138 An average reactivity between two values of conversion X_1 and X_2 was also defined:

$$r_{X_1-X_2} = \frac{\int_{t_{X_1}}^{t_{X_2}} \frac{r(t)dt}{1-X(t)}}{t_{X_2} - t_{X_1}}. \tag{5}$$

139 There is no standardized definition for the reactivity [41]. In this study, the average reactivity
140 was calculated between 1 and 80% conversion as in several investigations in literature

[16,19,41]. This choice allowed to obtain a trend that was not affected by the particular phenomena that can occur at high conversion values.

Additionally, the derivative thermogravimetric (DTG) curve was obtained with the following equation:

$$DTG(t_n) = -\frac{m_{n+1} - m_{n-1}}{t_{n+1} - t_{n-1}}. \quad (6)$$

where t_{n-1}, t_n and t_{n+1} are consecutive time steps, m_{n-1} is the mass measured at time t_{n-1} and m_{n+1} is the mass measured at time t_{n+1}.

To allow comparison between the different samples, results from pyrolysis and gasification of samples with added K_2CO_3 (mixtures and without contact) were corrected by subtracting the equivalent mass profiles of pure K_2CO_3 to the measured mass profiles. An example is given in **Figure 2**. The black curve is the mass as directly measured in TGA. The orange curve is the pure K_2CO_3 profile that is subtracted. Finally, the blue curve is the equivalent char mass with the K_2CO_3 subtracted. It is this last mass that is used in further data treatments and interpretations.

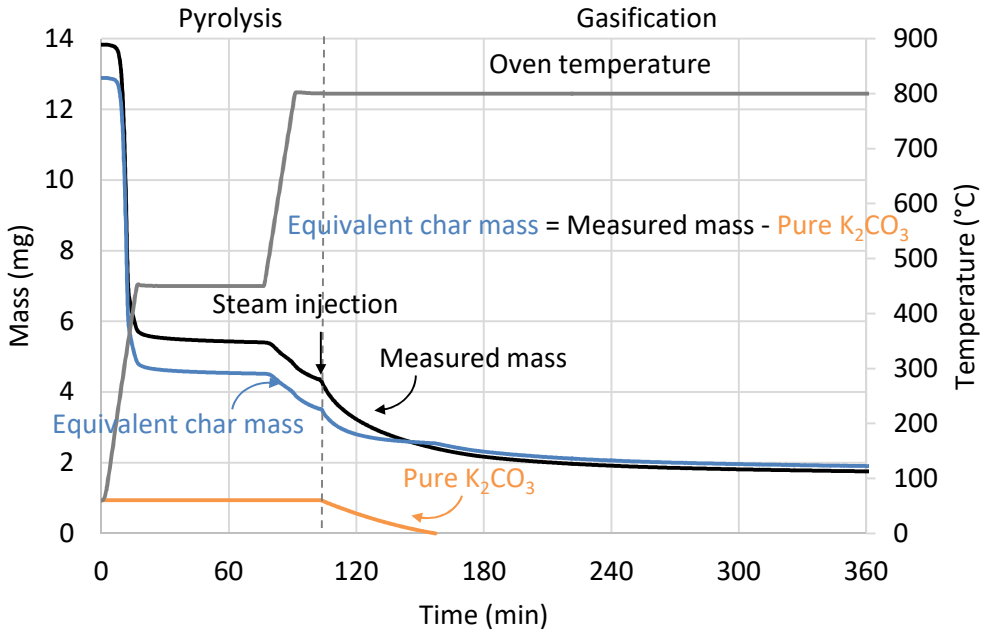

Figure 2. Measured mass, equivalent char mass (as used in further interpretations) and corresponding pure K_2CO_3 mass.

2.3. Characterization techniques

2.3.1. Optical microscopy

Optical microscopy was used to observe the sample morphology before and after reaction. An Olympus SZX12 microscope was used with a ToupTek Photonics ToupCam camera and the associated ToupView software.

2.3.2. Scanning electron microscopy coupled to energy dispersive X-ray spectroscopy

Scanning electron microscopy coupled to energy dispersive X-ray spectroscopy (SEM–EDX) was used to study the morphology and the surface elemental composition of the TGA residues. A Philips XL30 microscope was used with a 15 kV electron beam. Back-scattered electrons (BSE) detection was used. It creates a contrast related to atomic number. Samples were placed on graphite tape and graphitized before analysis.

2.4. Thermodynamic equilibrium simulation method

Calculations at thermodynamic equilibrium were performed to simulate the behavior of K_2CO_3 under steam at 800 °C.

They were performed by minimization of the Gibbs free energy of the total system with the FactSage 7.2 software and the databases FTsalt and FactPS [42,43].

The steam gasification procedure applied to pure K_2CO_3 was simulated at thermodynamic equilibrium. The initial data are listed in **Table 2**. K_2CO_3 initial mass was slightly different from the experimental initial mass put in the TGA since calculations dealt with the gasification step and there was a slight mass loss before gasification (**Figure 4**).

The gas flow is constant, therefore the effect of time is simulated by the effect of the initial gas mass [44].

Table 2. Initial data for the thermodynamic equilibrium calculations.

Temperature	800 °C
Initial solid	K_2CO_3 0.54 mg 0.70 mg 1.23 mg 1.73 mg 2.99 mg
Initial gas	0 to 1.5 g N_2 + 0 to 0.241 g H_2O (0.5 $L.min^{-1}$, 0 to 30 min)

3. Results and Discussion

3.1. Pure biomass steam gasification

The results obtained during the pyrolysis and steam gasification of the pure biomass samples are plotted in **Figure 3**.

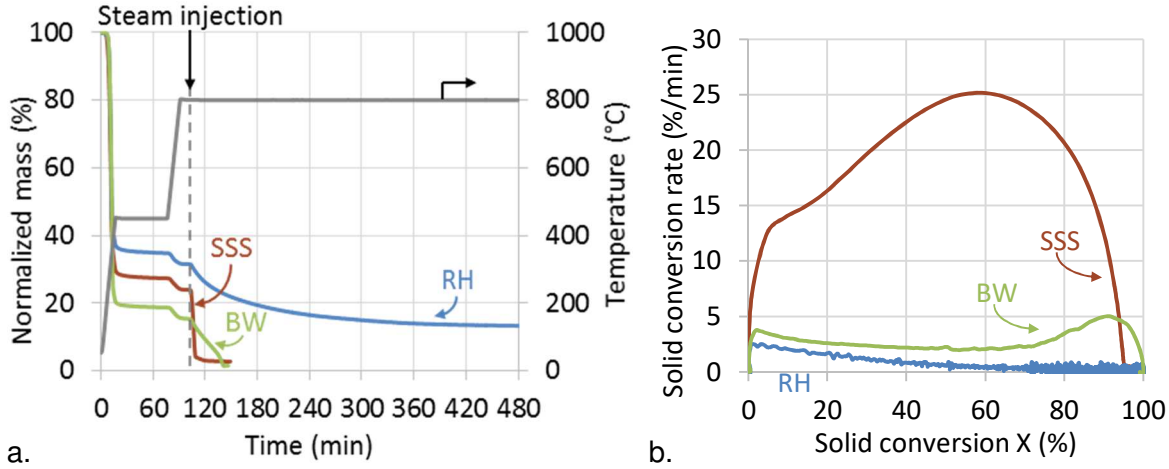

Figure 3. TGA of rice husks (RH), sunflower seed shells (SSS) and beech wood (BW) presented as a. normalized mass versus time and b. gasification solid conversion rate versus gasification solid conversion.

The three biomass species show similar behaviors during pyrolysis. Significant mass loss occurs below 450 °C, in agreement with literature [45]. Then significantly different behaviors are observed during gasification. More than six hours are required to gasify rice husks

(average reactivity $r_{1\text{-}80\%}$ = 1.4%.min^{-1}) while gasification of sunflower seed shells require less than 20 minutes (average reactivity $r_{1\text{-}80\%}$ = 30.3%.min^{-1}). Rice husks gasification rate is continuously decreasing whereas sunflower seed shells has a constant and then decreasing conversion rate. Beech wood has an intermediate behavior with a gasification time of around 40 minutes (average reactivity $r_{1\text{-}80\%}$ = 4.9%.min^{-1}) and a gasification rate that is constant and then increases. Another work showed that these significant differences are mainly due to the inorganic composition of the biomass species, and not to the char physical properties [46].

3.2. Pure K_2CO_3 thermogravimetric analysis (TGA)

The pyrolysis and gasification procedure was applied to various mass samples of K_2CO_3. **Figure 4** shows the mass evolution versus time.

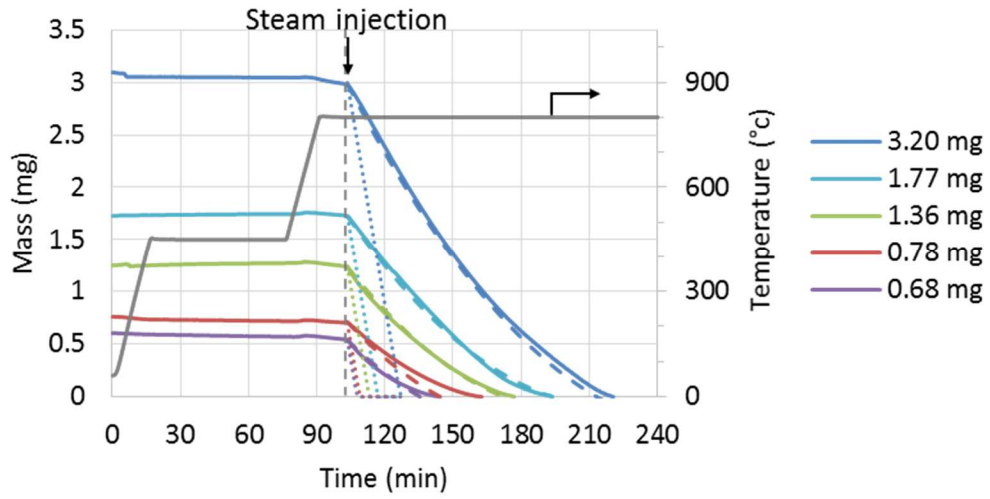

Figure 4. Mass evolution versus time of various initial masses of K_2CO_3 alone during the pyrolysis and gasification procedure. Full line: measurement. Dotted line: thermodynamic equilibrium simulation. Dashed line: mathematical model fitting experimental data.

A very low volatilization of K_2CO_3 is observed during the pyrolysis step. On the contrary, the sample is completely volatilized when steam is injected. This behavior is in accordance with

209 literature [47–49]. The volatilization time depends on the initial mass varying from 40 min to
210 2h for samples between 0.68 and 3.20 mg.

211 In order to explain this behavior, a thermodynamic equilibrium simulation with pure K_2CO_3
212 was conducted. Under thermodynamic equilibrium conditions, in the case where K_2CO_3 is in
213 an inert atmosphere, it is slightly volatilized as K(g) and CO_2(g). On the opposite, in the case
214 where K_2CO_3 is in a steam atmosphere, it is largely volatilized as KOH(g). These volatilized
215 species can be explained by the following reactions [50,51]:

$$K_2CO_3(s) = 2\,K(g) + CO_2(g) + 0.5\,O_2(g) \quad (7)$$

$$K(g) + H_2O(g) = KOH(g) + 0.5\,H_2(g) \quad (8)$$

216 The simulated mass evolution of K_2CO_3 during the gasification step is plotted in dotted lines
217 in **Figure 4**. The simulation predicts that the whole amount of K_2CO_3 volatilizes in 2 to 20
218 minutes in thermodynamic equilibrium conditions. It shows mass transfer limitations during
219 K_2CO_3 volatilization. They could be due to the configuration of the crucible in the carrier gas
220 and/or to the K_2CO_3 particle size.

221 The mass evolution of K_2CO_3 as a function of time and initial mass was modeled through a
222 second-degree polynomial of general equation as shown in **Figure 4**. The model is
223 presented in Supplementary Material. Here, the objective was only to fit experimental results
224 in the TGA configuration to be able to extrapolate the results to other initial masses in the
225 studied range. It has not been attempted in the present work to give a signification to these
226 coefficients as in the literature [48]. For example, Knudsen *et al.* [48] have modelled the
227 evaporation of pure K-compounds based on mass transfer for a carrier gas sweeping the
228 crucible parallel to its surface, on the contrary to the TGA configuration where the gas is
229 perpendicular. Authors have assumed K transport was controlled by diffusion through an
230 external gas film. They have used mass transfer correlations to obtain the coefficients.

3.3. Interactions between materials

Pyrolysis and gasification of rice husks—slow-gasifying biomass—were carried out with K_2CO_3 added in two configurations: mixed and without contact in a divided crucible. Both configurations had approximately the same proportion of added K_2CO_3, i.e. 7 wt%. This proportion corresponds to 4 wt% of K in the initial mixture (**Table 1**). Such a high content (see natural contents < 1 wt% of K in raw biomass, in **Table 1**) was selected to clearly observe the phenomena. Results were compared to rice husks and sunflower seed shells alone. The evolution with time of the normalized mass of the samples—including ashes—and the DTG curves are presented in **Figure 5**. As stated in the Materials and Methods section (section 2.2), the measured mass profiles were corrected by subtracting the equivalent mass profiles of pure inorganic compound.

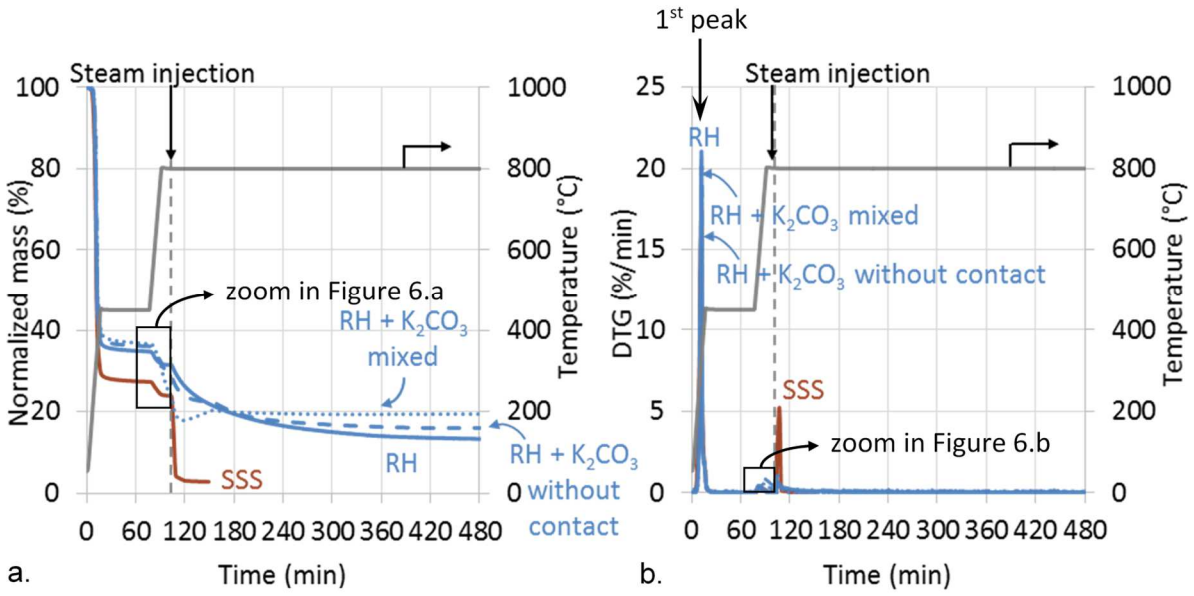

Figure 5. a. TGA and b. DTG of RH with and without added K_2CO_3 and of SSS.

The apparent difference between the two biomass species during low temperature pyrolysis is due to the difference of ash content. When looking at the DTG curves it can be seen that all samples with and without K_2CO_3 have the same behavior during low temperature pyrolysis, i.e. a first very high peak below 450 °C (**Figure 5**.b). It corresponds to the degradation of the biomass macromolecular constituents [52].

Above 450 °C, the curves indicate that K_2CO_3 addition has an effect on both pyrolysis and gasification steps. This effect is discussed in the following sections.

3.3.1. Influence of K_2CO_3 addition on the pyrolysis reaction

Though the present study focuses on the gasification reaction, an effect of K addition already appeared during the pyrolysis step at high temperature, before steam injection. Since the char formed during pyrolysis is the starting material of the gasification reaction, it is important to also investigate these phenomena.

3.3.1.1. High temperature pyrolysis phenomena observation

Figure 6 is a zoom of the high temperature pyrolysis from **Figure 5**. It shows the evolution of the normalized mass and DTG of the samples during the 30 minutes preceding steam injection, i.e. during heating from 450 to 800 °C.

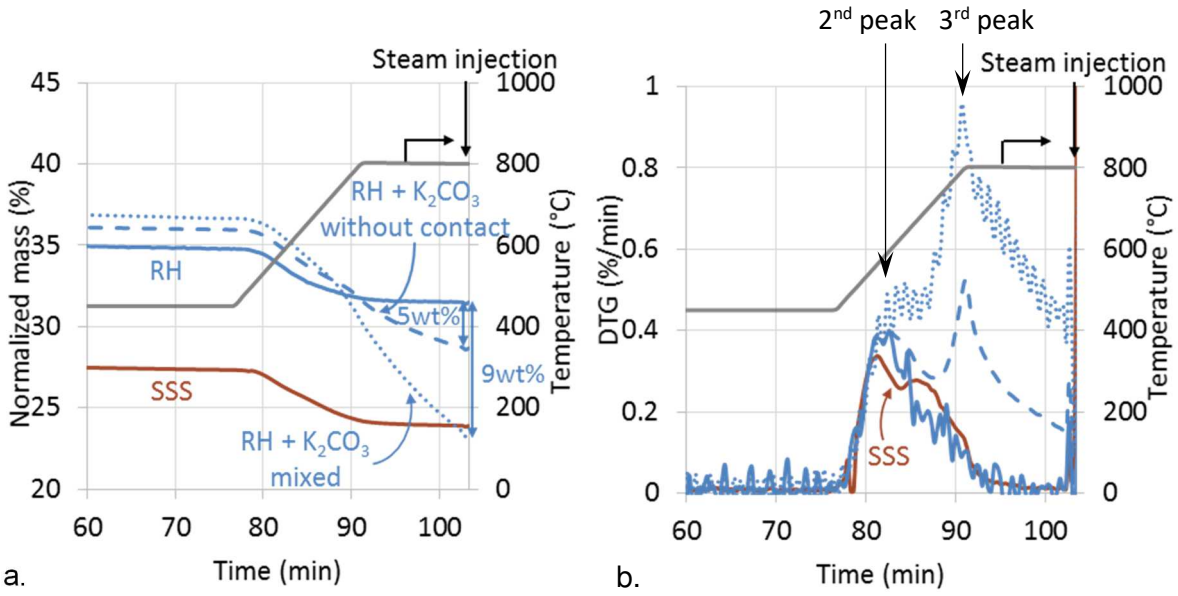

Figure 6. a. TGA and b. DTG of RH with and without added K_2CO_3 and of SSS. Zoom on the high temperature pyrolysis. Full line: alone. Dotted line: mixed. Dashed line: without contact. Oscillations observed in b. are due to the experimental set-up and are considered as not significant.

Above 450 °C, a second DTG peak is observed around 82 min and 500 °C for all samples with and without added K_2CO_3. It corresponds to the typical mass loss observed when heating the samples between 450 and 800 °C, as seen with pure biomass, and is due to a residual char devolatilization.

However, when K_2CO_3 is added to rice husks (mixed and without contact), a third DTG peak is observed close to the beginning of the 800 °C holding time. An additional experiment where heating is conducted up until 1000 °C instead of 800 °C shows that the peak is maximum around 860 °C (see Supplementary materials). The effect is stronger when K_2CO_3 is mixed with rice husks. Nevertheless, it appears even if rice husks are not in contact with the added K_2CO_3 which means it is related to the gas phase and probably attributed to K volatilization. The stronger effect in the case of the mixture can then be explained by a higher concentration of K-compound in the gas layer around the biomass in this case.

3.3.1.2. Third DTG peak investigation during pyrolysis step

In order to determine the origin of this third DTG peak, the same experiment was conducted on rice husks with K_2CO_3 added without contact but it was stopped after the pyrolysis step at 800 °C, i.e. before steam injection. Optical microscope observations of the crucible before and after the experiment are presented in **Figure 7**.

a. 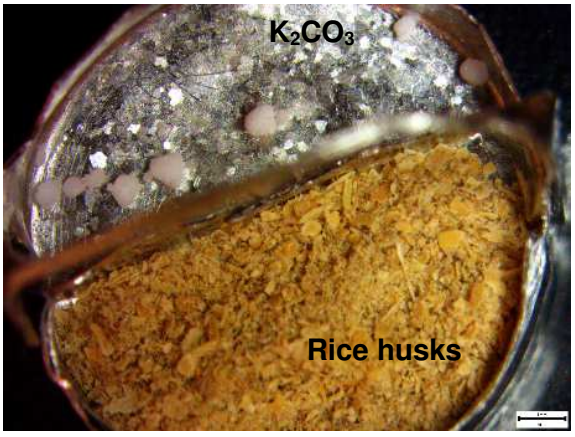

b. 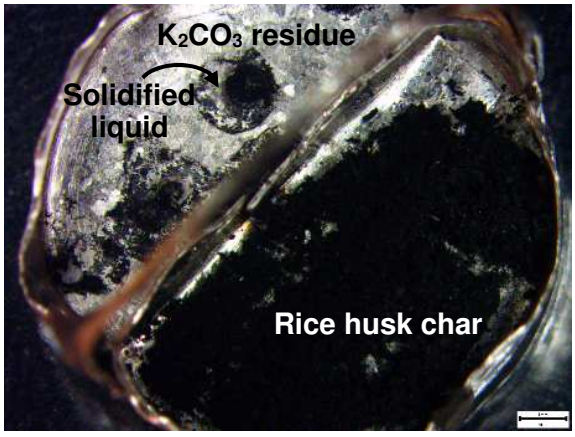

Figure 7. RH with K_2CO_3 added without contact a. before and b. after pyrolysis until 800 °C in the TGA, i.e. procedure stopped before steam injection.

Rice husk chars have no visual particularity at this scale. On the K_2CO_3 side, grains which were initially white are covered with a black layer after pyrolysis until 800 °C and material under each grain suggests a partial fusion. The black layer most likely is carbon deposited on top of the inorganic residue. These observations are in agreement with literature where higher char yields have been observed with K impregnation due to condensation of tars [53–55]. However, a competition between this char formation and tar cracking have been noted [54]. Regarding the residue under the black layer, it cannot be pure K_2CO_3 (whose melting point is 901°C [42] i.e. above the pyrolysis temperature) but a material with a lower melting point. Since liquid formation is associated to a higher volatilization, it is in agreement with the fact that the third DTG peak also occurs before the pure K_2CO_3 melting point. These results indicate that a reaction occurs on the K_2CO_3 side when it is in presence of biomass, even without contact.

It is known that pyrolysis gases (CO_2, H_2O, CO, H_2) and inorganic gases (H_2S, NH_3, HCl, KCl, etc.) are released during biomass devolatilization [56,57]. Therefore, the liquid observed at 800 °C could be due to the reaction of K_2CO_3 with one of these gases.

The residue at 800 °C on the K_2CO_3 side was analyzed by SEM-EDX and only K, C and O were detected. H cannot be detected by this methods.

Therefore K_2CO_3 most likely reacts with H_2O(g) originating from biomass devolatilization. The residue is then a mixture of K_2CO_3 and KOH where a core of K_2CO_3 is at equilibrium with a liquid phase (solidified at ambient temperature).

The K_2CO_3-KOH phase diagram (see Supplementary Material) predicts that, at 800 °C, solid K_2CO_3 is in equilibrium with a liquid for compositions up to 23.5mol% KOH. This is a reasonable composition that could have been obtained from the reaction with H_2O(g) from the biomass devolatilization. It also predicts that a liquid phase can appear at 450 °C, the temperature of the first plateau of the TGA procedure. This behavior has been confirmed by

an additional experiment where a higher mass loss of K_2CO_3 was observed during high temperature pyrolysis after it had been in contact with steam during the 450 °C plateau than when it had only been in a N_2 atmosphere (see Supplementary Material).

Therefore, from these results, the third DTG peak can be attributed to the devolatilization of the carbon matrix catalyzed by a K-compound, probably, KOH(g), released to the gas phase from the K_2CO_3 side of the crucible.

In literature, authors do not usually conduct pyrolysis at such high temperatures. Indeed, as previously stated, the main mass loss occurs below 450 °C so studies are focused on that temperature range. However, studies in the carbon activation literature [58] are in accordance with the results from the present work where pyrolysis at high temperature in the presence of a K-compound induces an additional mass loss, i.e. third DTG peak. However, in the case of activated carbons the K-compound is added through impregnation of an aqueous solution, or occasionally through dry mixing (Amoco process) [58], whereas in the present study the effects are observed including when K_2CO_3 is not in contact with the biomass.

For the first time it is here demonstrated that the effect occurs through the gas phase. The main explanation given in literature regarding the mechanism of action involves the intercalation of K followed by its explosive removal to form the pores [58].

3.3.2. Influence of K_2CO_3 addition on the gasification reaction

3.3.2.1. Gasification phenomena observation

Figure 8 shows the gasification solid conversion and conversion rate of rice husks with and without added K_2CO_3 compared to that of sunflower seed shells. It is clearly seen that, K_2CO_3 has an effect on the gasification step.

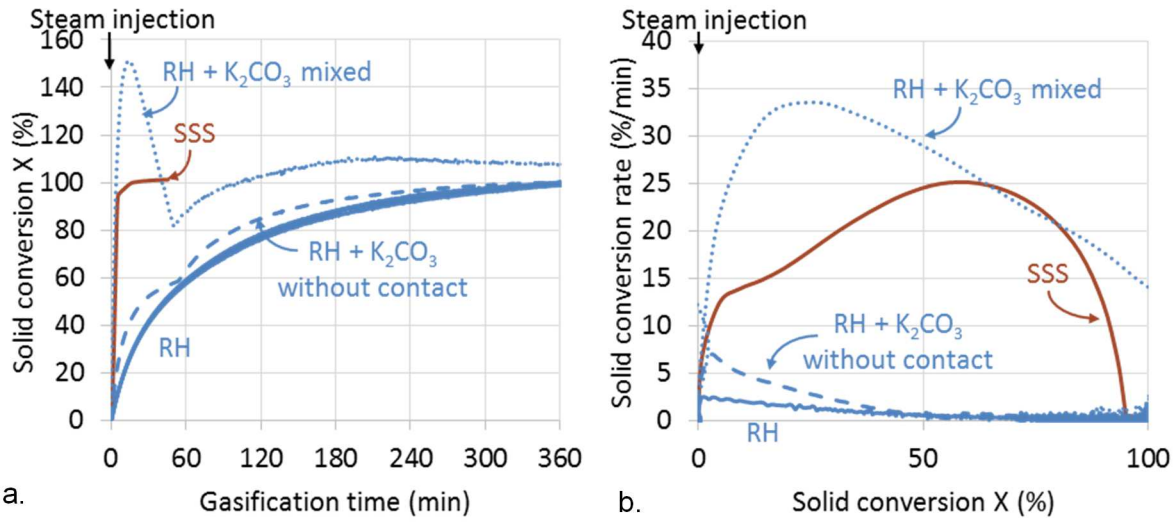

Figure 8. Gasification at 800°C of RH with and without added K_2CO_3 and of SSS. a. Solid conversion as a function of time (for RH alone, three replicates are plotted which explains the apparent large line). b. Solid conversion rate as a function of the conversion.

As stated in the Materials and Methods section (see 2.2), the results were corrected by subtracting the equivalent mass profiles of pure K_2CO_3 to the measured mass profiles of the total sample. Therefore, if the rice husks and K_2CO_3 behaviors were independent, their mass profiles would have been additive and the presented equivalent mass profile of rice husks would have been similar to rice husks alone. Yet, the conversion profile of the sample of rice husks and K_2CO_3 mixed goes above 100%. These high values, which are not physically possible, occur around the time where the profile of pure K_2CO_3 is subtracted. It means that it is an effect of the mathematical treatment of the data, i.e. of the K_2CO_3 profile subtraction, and not a measured effect. In addition, both samples with added K_2CO_3, mixed and without contact, have a sudden slope change approximately 50 min after steam injection, which corresponds to the completion of the pure K_2CO_3 volatilization that is subtracted to the results. Moreover, both curves are above the curve of rice husks alone. This last difference compared to the curve of rice husks alone is significant even in the case where K_2CO_3 is added without contact. Indeed, **Figure 8**.a shows three replicates of the experiments on rice

351 husks alone that are all grouped compared to curves with added K_2CO_3. All the above
352 observations show that there is an interaction between the biomass and the inorganic
353 sample both when K_2CO_3 is mixed and without contact. The behaviors of the samples cannot
354 be assessed through the simple addition of the behaviors of the pure rice husks and K_2CO_3.
355 This means that the equivalent rice husks profiles presented do not represent the real mass
356 loss on the rice husks side. Therefore, quantitative assumptions cannot be drawn from these
357 data but trends still can be analyzed.

358 When comparing the addition mode of K_2CO_3, it can be seen that mixing induces a stronger
359 catalytic effect during gasification. However, even if it is weak, the effect of K_2CO_3 without
360 contact with rice husks is present. This demonstrates that it acts, at least partially, through
361 the gas phase. The stronger effect in the case of the mixture can then be explained by a
362 higher concentration of K-compound in the gas layer around the biomass in this case.

363 **3.3.2.2. Influence of the pyrolysis step on gasification**

364 An additional experiment was designed in order to check if a reaction during pyrolysis
365 influences the behavior during gasification. Pyrolysis of rice husks with added K_2CO_3 without
366 contact was carried out and the resulting char was gasified alone, after the residue on the
367 K_2CO_3 side was removed. Results are shown in **Figure 9**.

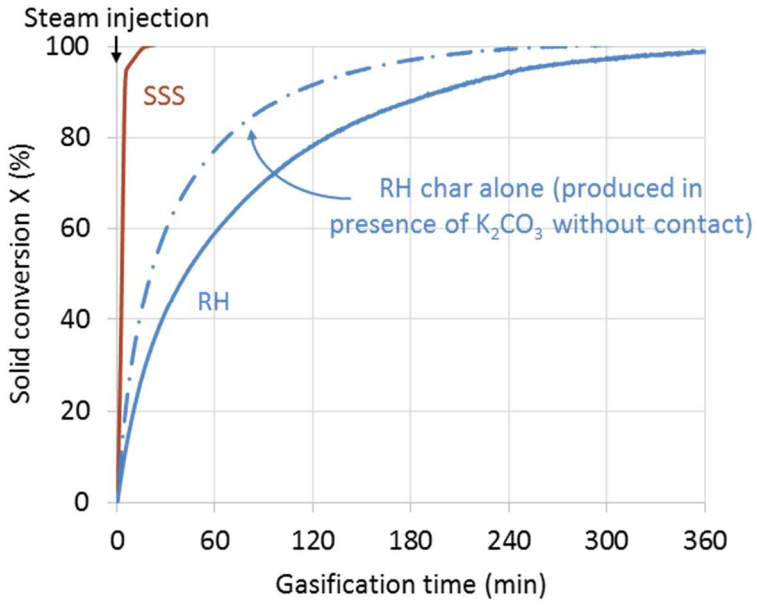

Figure 9. Gasification solid conversion as a function of time of RH char alone produced in presence of K_2CO_3 without contact, compared to pure RH and SSS alone.

During this experiment, only char was gasified, therefore no subtraction of a K_2CO_3 profile was required. This explains that the curve does not have the sudden slope change like the previous ones. It is seen directly that the gasification rate of rice husks is higher than for pure RH alone while K_2CO_3 is not present anymore during gasification. Its average reactivity between 1 and 80% conversion increased from 1.4 to 2.2 $\%.min^{-1}$. To our knowledge, this result has never been demonstrated in the literature. It indicates that the interaction between K_2CO_3 and char during the pyrolysis step catalyzes a subsequent gasification. Moreover, this effect occurs without contact between the biomass and the inorganic compound, therefore through the gas phase during pyrolysis step by the volatilization of K compounds and their condensation on the biomass char.

3.3.3. Ash characterization

3.3.3.1. Effects of K_2CO_3 addition on ash yield and ashes appearance

From the normalized mass profiles presented in **Figure 5**, it can be observed that when K_2CO_3 is added to rice husks, mixed or without contact, the mass stabilizes at a higher ash yield (19.7 and 15.2wt% respectively) than rice husks alone (13.6wt%) (**Table 3**).

Table 3. Gasification ash yield measured in TGA and associated theoretical yields.

	Rice husks	Rice husks + K_2CO_3 without contact	Rice husks + K_2CO_3 mixed
Added K_2CO_3 (wt%)	—	7.0 ± 0.3	
Experimental (wt%)	13.6 ± 0.5	15.2 ± 0.7	19.7 ± 1.3
Theoretical if all K_2O remains* (wt%)	—	17.4 ± 0.8	
Theoretical if all K_2CO_3 remains** (wt%)	—	19.6 ± 0.8	

* $Ash_{with\ K2O} = \%K_2CO_3 \times \frac{M_{K2O}}{M_{K2CO3}} + (100 - \%K_2CO_3) \times Ash_{rice\ husks}$

** $Ash_{with\ K2CO3} = \%K_2CO_3 + (100 - \%K_2CO_3) \times Ash_{rice\ husks}$

This higher ash yield suggests that at least a part of the added K_2CO_3 is incorporated to the biomass char and therefore to the biomass ash at the end of the gasification step. The increase is observed including in the case of addition without contact. Therefore, this proves that K_2CO_3 is incorporated after its volatilization during the pyrolysis step. As a result, the K-species in the ash can be in another form than directly K_2CO_3, such as K_2O. The higher ash yield value corresponds to the theoretical ash yield calculated if all the added K_2CO_3 is incorporated to the ashes, either directly as K_2CO_3 (19.6wt%) or as K_2O (17.4wt%).

In order to investigate this supposed reaction of a K-species with the rice husk ashes, the ashes from the previous experiments were characterized through optical microscope and SEM-EDX.

Pictures from microscope observation of ashes from rice husks alone and mixed with K_2CO_3 are presented **Figure 10**.

a.  b. 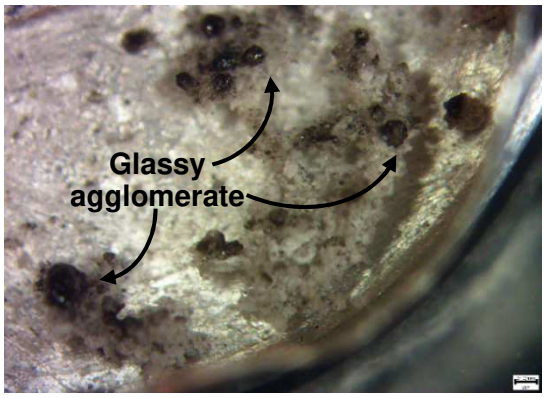

Figure 10. Ashes from pyrolysis and gasification of RH a. alone and b. with mixed K_2CO_3 (same aspect without contact).

Ashes in the presence of K_2CO_3 show some black glassy agglomerates on top of the white ashes (**Figure 10**.b) that are absent from rice husks alone (**Figure 10**.a). It suggests the formation at the process temperature of a liquid that solidified at ambient temperature. The SiO_2-K_2O phase diagram (see Supplementary Material) confirms that liquid can be present at the process temperature of 800 °C. The $SiO_2/(K_2O+SiO_2)$ ratio for a mixture of rice husks and 7wt% of K_2CO_3 is of 0.79 (from rice husks composition in **Table 1**). However, local concentrations could vary largely to reach lower or higher ratios. The change in appearance in the presence of K_2CO_3—including without contact—confirms that a reaction occurs between the added K_2CO_3 or one of its decomposition products and the inorganic compounds naturally contained in biomass—most likely SiO_2 which represents 94 wt% of the inorganic content of rice husks.

The same ashes were characterized through SEM-EDX, as presented in **Figure 11**.

415 a. 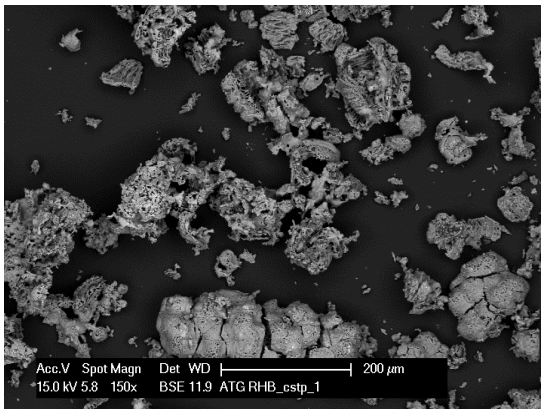

b. 

416 **Figure 11. SEM observation of ashes from pyrolysis and gasification of RH a. alone**
417 **and b. with K_2CO_3 added without contact (same aspect mixed).**

418 Again with SEM, the typical rice husk ashes and the glassy agglomerates can be
419 distinguished. The EDX analysis confirms that the typical rice husks ashes contain mainly
420 SiO_2. In the glassy agglomerates, the detected elements are K, Si and O. This supports the
421 idea of K-silicates formation.

422 This demonstrates that, in addition to influencing the pyrolysis and gasification of the
423 carbonaceous matrix, the added K_2CO_3 also reacts with the inorganic elements inherent to
424 the rice husks. This behavior is supported by literature observations of the reaction between
425 K-compounds and SiO_2 to form K-silicates [20,21,59]. However, our study suggests that the
426 reaction involves the gas phase, which has not been proved in literature.

427 This leads to a limitation of the catalysis of the gasification by K_2CO_3 due to its reaction on
428 SiO_2 inherent to the rice husks.

429 **3.3.3.2. Competing interactions of K with carbon and silica**

430 To demonstrate these competing interactions, the same experimental procedure was applied
431 to beech wood with K_2CO_3 added without contact. Beech wood had a very low SiO_2 content
432 so it was expected that K_2CO_3 would have induced a stronger catalysis than for rice husks.

The normalized mass evolution and the gasification conversion profiles are shown in **Figure 12** for beech wood alone and with K_2CO_3 without contact during pyrolysis and gasification.

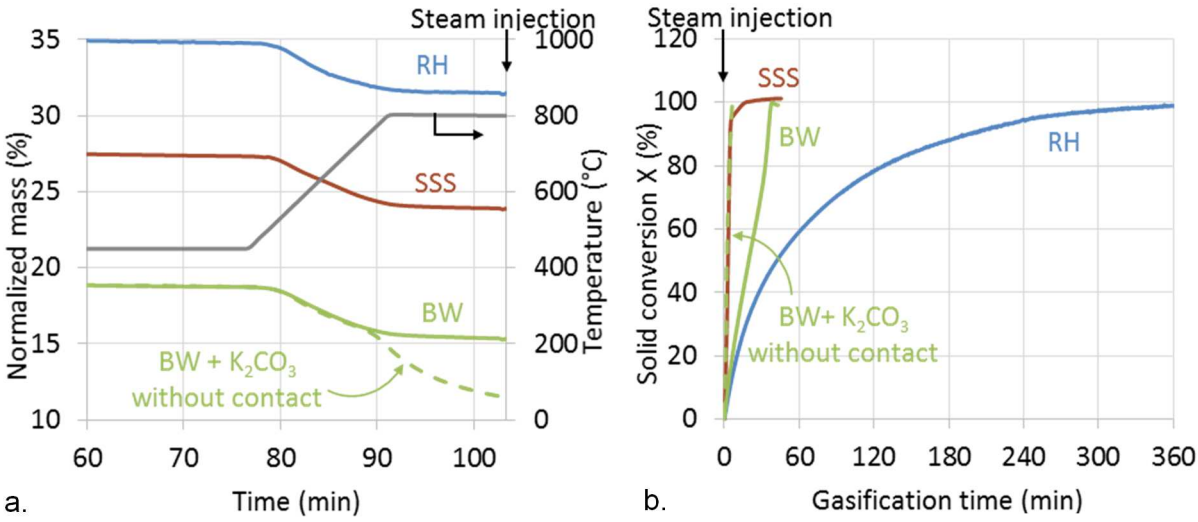

Figure 12. TGA of BW with and without added K_2CO_3 and of RH and SSS during a. the high temperature pyrolysis step and b. the steam gasification step.

The additional mass loss during high temperature pyrolysis (**Figure 12**.a) occurs for beech in the same way as for rice husks (third DTG peak).

Regarding gasification (**Figure 12**.b) when K_2CO_3 is added without contact, beech wood reactivity greatly increases (average reactivity increasing from $r_{1\text{-}80\%}$ = 4.9 to 42.4%min^{-1}). It reaches sunflower seed shells level ($r_{1\text{-}80\%}$ = 30.3%.min^{-1}). The catalysis is very strong compared to what is observed in the case of rice husks (average reactivity increasing from $r_{1\text{-}80\%}$ = 1.4 to 2.2 %.min^{-1}). As stated previously, beech has very low ash and Si contents while rice husks is a Si-rich biomass. Therefore it confirms that the competing reaction of K_2CO_3 decomposition product on the inherent SiO_2 prevents it to catalyze the gasification.

4. Synthesis of the several effects of K along biomass pyrolysis and steam gasification

During the present investigation, we have observed that the addition of K during the pyrolysis and gasification of rice husks has significant effects at several levels. It influences the kinetics of both pyrolysis and gasification steps and it interacts with the inorganic compounds inherent to the biomass.

It is important to note that all these effects occur whether K_2CO_3 is in contact or not with the biomass. This behavior highlights the fact that K_2CO_3 mechanisms of action are through the gas phase, with the formation of KOH(g). This is permitted by the fact that experiments use a low gas flow that enables the mass transfers and reactions to occur at the proximity of the crucible. Conducting experiments with a high gas flow would then be expected to reduce or suppress the catalytic effect which would confirm this result. Effects observed in the case of mixtures are stronger than without contact which can be explained by a higher concentration of K-compound in the gas layer around the biomass in this case.

The effects of K_2CO_3 on biomass pyrolysis and gasification demonstrated in the present study are summarized in **Figure 13**. During the pyrolysis, steam is produced and reacts with K_2CO_3 to form a mixture of K_2CO_3 and KOH where a core of K_2CO_3 is at equilibrium with a liquid phase. When the pyrolysis reaches a high temperature, $KOH_{(g)}$ is volatilized from this mixture and catalyzes an additional devolatilization of the char. Then, when steam is added, the mixture completely volatilizes as $KOH_{(g)}$. This formed $KOH_{(g)}$ catalyzes the gasification and reacts with the biomass inherent SiO_2 to form K-silicates.

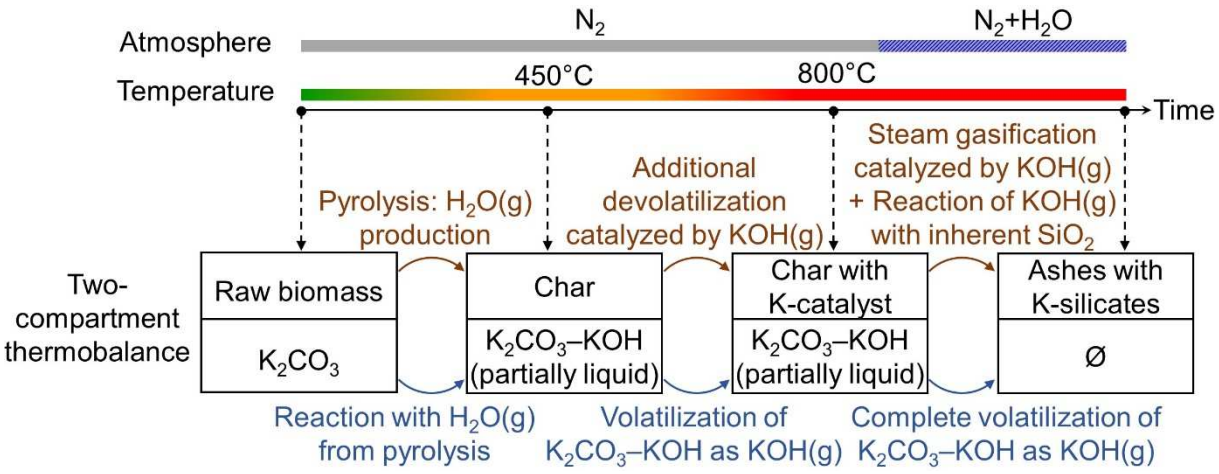

Figure 13. Scheme of the effects of K_2CO_3 on biomass pyrolysis and gasification, in the case of K_2CO_3 added without contact.

It is demonstrated that the interaction of K_2CO_3 with the biomass during the pyrolysis is decisive for the subsequent gasification. Indeed, when the two materials are in presence only during pyrolysis but not during gasification, catalysis is still observed.

However, the catalytic effect remains weaker than what has been observed in literature in the case of impregnation or occasionally mixing [32,35,60]. This is attributed to the fact that the present work intends to catalyze rice husks that have a high content in Si, while most literature studies work with materials with a low ash content [4,6,9–12,33,34,36]. Hence, we have confirmed this fact by experiments on beech wood that has a very low Si content. Along with the ash characterization during the TGA experiments, these results highlight a competition between on the one hand the influence of K_2CO_3 on the biomass pyrolysis and char gasification kinetics and on the other hand its interaction with SiO_2 inherent to the rice husks.

5. Conclusions

The present work contributes to the understanding of the K role in biomass steam gasification. It has demonstrated the competition between SiO_2 and the carbonaceous matrix to react with a K-catalyst. On the one hand, the K-compound catalyzes the high temperature

pyrolysis and the steam gasification of the carbonaceous matrix of biomass. On the other hand, its decomposition product reacts with the SiO_2 inherent to biomass. In both cases, effects are observed including when the K-compound is not in direct contact with the biomass which demonstrates that the mechanisms of action involve the gas phase.

During the pyrolysis at high temperature, an additional mass loss occurs in presence of K_2CO_3. This observation is in accordance with the carbon chemical activation literature. It has been demonstrated in the present work that it is related to an additional volatilization of the carbon matrix in relation with the formation of KOH(g). The latter is formed from the reaction of $K_2CO_3$with H_2O(g) released from the devolatilization of the carbon matrix.

Regarding the gasification step itself, K_2CO_3 increases the reaction rate both with and without contact with the biomass. It has been demonstrated in the present study that the interaction of K_2CO_3 with the biomass during the pyrolysis step is decisive for the ulterior gasification.

Acknowledgements

The authors would like to thank Sébastien THIERY for his help with TGA experiments.

Funding

This research was funded by the Agence de l'Environnement et de la Maîtrise de l'Energie.

References

[1] Vassilev SV, Baxter D, Andersen LK, Vassileva CG. An overview of the chemical composition of biomass. Fuel 2010;89:913–33. https://doi.org/10.1016/j.fuel.2009.10.022.

[2] Bartels M, Lin W, Nijenhuis J, Kapteijn F, van Ommen JR. Agglomeration in fluidized beds at high temperatures: Mechanisms, detection and prevention. Prog Energy Combust Sci 2008;34:633–66. https://doi.org/10.1016/j.pecs.2008.04.002.

[3] Sikarwar VS, Zhao M, Clough P, Yao J, Zhong X, Memon MZ, et al. An overview of advances in biomass gasification. Energy Environ Sci 2016;9:2939–77. https://doi.org/10.1039/C6EE00935B.

[4] Huang Y, Yin X, Wu C, Wang C, Xie J, Zhou Z, et al. Effects of metal catalysts on CO2 gasification reactivity of biomass char. Biotechnol Adv 2009;27:568–72. https://doi.org/10.1016/j.biotechadv.2009.04.013.

[5] Yip K, Tian F, Hayashi J, Wu H. Effect of Alkali and Alkaline Earth Metallic Species on Biochar Reactivity and Syngas Compositions during Steam Gasification. Energy Fuels 2009;24:173–181.

[6] Zhang Y, Ashizawa M, Kajitani S, Miura K. Proposal of a semi-empirical kinetic model to reconcile with gasification reactivity profiles of biomass chars. Fuel 2008;87:475–81. https://doi.org/10.1016/j.fuel.2007.04.026.

[7] Arnold RA, Hill JM. Catalysts for gasification: a review. Sustain Energy Fuels 2019;3:656–72. https://doi.org/10.1039/C8SE00614H.

[8] Nzihou A, Stanmore B, Sharrock P. A review of catalysts for the gasification of biomass char, with some reference to coal. Energy 2013;58:305–17. https://doi.org/10.1016/j.energy.2013.05.057.

[9] Bouraoui Z, Dupont C, Jeguirim M, Limousy L, Gadiou R. CO2 gasification of woody biomass chars: The influence of K and Si on char reactivity. Comptes Rendus Chim 2016;19:457–65. https://doi.org/10.1016/j.crci.2015.08.012.

[10] Kramb J, Gómez-Barea A, DeMartini N, Romar H, Doddapaneni TRKC, Konttinen J. The effects of calcium and potassium on CO2 gasification of birch wood in a fluidized bed. Fuel 2017;196:398–407. https://doi.org/10.1016/j.fuel.2017.01.101.

[11] Lahijani P, Zainal ZA, Mohamed AR, Mohammadi M. CO2 gasification reactivity of biomass char: Catalytic influence of alkali, alkaline earth and transition metal salts. Bioresour Technol 2013;144:288–95. https://doi.org/10.1016/j.biortech.2013.06.059.

[12] Kramb J, DeMartini N, Perander M, Moilanen A, Konttinen J. Modeling of the catalytic effects of potassium and calcium on spruce wood gasification in CO2. Fuel Process Technol 2016;148:50–9. https://doi.org/10.1016/j.fuproc.2016.01.031.

[13] Hüttinger KJ, Minges R. Influence of the catalyst precursor anion in catalysis of water vapour gasification of carbon by potassium: 1. Activation of the catalyst precursors. Fuel 1986;65:1112–21. https://doi.org/10.1016/0016-2361(86)90179-1.

[14] Hüttinger KJ, Minges R. The influence of the catalyst precursor anion in catalysis of water vapour gasification of carbon by potassium: 2. Catalytic activity as influenced by activation and deactivation reactions. Fuel 1986;65:1122–8. https://doi.org/10.1016/0016-2361(86)90180-8.

[15] DeGroot WF, Kannan MP, Richards GN, Theander O. Gasification of agricultural residues (biomass): influence of inorganic constituents. J Agric Food Chem 1990;38:320–3. https://doi.org/10.1021/jf00091a070.

[16] Dupont C, Nocquet T, Da Costa JA, Verne-Tournon C. Kinetic modelling of steam gasification of various woody biomass chars: Influence of inorganic elements. Bioresour Technol 2011;102:9743–8. https://doi.org/10.1016/j.biortech.2011.07.016.

[17] Dupont C, Jacob S, Marrakchy KO, Hognon C, Grateau M, Labalette F, et al. How inorganic elements of biomass influence char steam gasification kinetics. Energy 2016;109:430–5. https://doi.org/10.1016/j.energy.2016.04.094.

[18] González-Vázquez MP, García R, Gil MV, Pevida C, Rubiera F. Unconventional biomass fuels for steam gasification: Kinetic analysis and effect of ash composition on reactivity. Energy 2018;155:426–37. https://doi.org/10.1016/j.energy.2018.04.188.

[19] Hognon C, Dupont C, Grateau M, Delrue F. Comparison of steam gasification reactivity of algal and lignocellulosic biomass: Influence of inorganic elements. Bioresour Technol 2014;164:347–53. https://doi.org/10.1016/j.biortech.2014.04.111.

[20] Kannan MP, Richards GN. Gasification of biomass chars in carbon dioxide: dependence of gasification rate on the indigenous metal content. Fuel 1990;69:747–53. https://doi.org/10.1016/0016-2361(90)90041-N.

564 [21] Link S, Arvelakis S, Hupa M, Yrjas P, Külaots I, Paist A. Reactivity of the Biomass
565 Chars Originating from Reed, Douglas Fir, and Pine. Energy Fuels 2010;24:6533–9.
566 https://doi.org/10.1021/ef100926v.
567 [22] López-González D, Fernandez-Lopez M, Valverde JL, Sanchez-Silva L. Gasification of
568 lignocellulosic biomass char obtained from pyrolysis: Kinetic and evolved gas analyses.
569 Energy 2014;71:456–67. https://doi.org/10.1016/j.energy.2014.04.105.
570 [23] Romero Millán LM, Sierra Vargas FE, Nzihou A. Steam gasification behavior of tropical
571 agrowaste: A new modeling approach based on the inorganic composition. Fuel
572 2019;235:45–53. https://doi.org/10.1016/j.fuel.2018.07.053.
573 [24] Strandberg A, Holmgren P, Wagner DR, Molinder R, Wiinikka H, Umeki K, et al. Effects
574 of Pyrolysis Conditions and Ash Formation on Gasification Rates of Biomass Char.
575 Energy Fuels 2017;31:6507–14. https://doi.org/10.1021/acs.energyfuels.7b00688.
576 [25] Feng D, Zhao Y, Zhang Y, Sun S, Gao J. Steam Gasification of Sawdust Biochar
577 Influenced by Chemical Speciation of Alkali and Alkaline Earth Metallic Species.
578 Energies 2018;11:205. https://doi.org/10.3390/en11010205.
579 [26] Jiang L, Hu S, Xu K, Wang Y, Syed-Hassan SSA, Su S, et al. Formation, fates and
580 roles of catalytic precursors generated from the K2CO3-carbon interactions in the
581 K2CO3-catalyzed CO2 gasification of coal char. J Anal Appl Pyrolysis 2017;124:384–
582 92. https://doi.org/10.1016/j.jaap.2016.11.006.
583 [27] Lv X, Xiao J, Shen L, Zhou Y. Experimental study on the optimization of parameters
584 during biomass pyrolysis and char gasification for hydrogen-rich gas. Int J Hydrog
585 Energy 2016;41:21913–25. https://doi.org/10.1016/j.ijhydene.2016.09.200.
586 [28] Zahara ZF, Kudo S, Daniyanto, Ashik UPM, Norinaga K, Budiman A, et al. CO2
587 Gasification of Sugar Cane Bagasse: Quantitative Understanding of Kinetics and
588 Catalytic Roles of Inherent Metallic Species. Energy Fuels 2018;32:4255–68.
589 https://doi.org/10.1021/acs.energyfuels.7b03147.

590 [29] Arnold RA, Habibi R, Kopyscinski J, Hill JM. Interaction of Potassium and Calcium in
591 the Catalytic Gasification of Biosolids and Switchgrass. Energy Fuels 2017;31:6240–7.
592 https://doi.org/10.1021/acs.energyfuels.7b00972.
593 [30] Bach-Oller A, Fursujo E, Umeki K. Effect of potassium impregnation on the emission of
594 tar and soot from biomass gasification. Energy Procedia 2019;158:619–24.
595 https://doi.org/10.1016/j.egypro.2019.01.164.
596 [31] DeGroot WF, Shafizadeh F. Kinetics of gasification of Douglas Fir and Cottonwood
597 chars by carbon dioxide. Fuel 1984;63:210–6. https://doi.org/10.1016/0016-
598 2361(84)90039-5.
599 [32] Feng D, Zhao Y, Zhang Y, Xu H, Zhang L, Sun S. Catalytic mechanism of ion-
600 exchanging alkali and alkaline earth metallic species on biochar reactivity during
601 CO2/H2O gasification. Fuel 2018;212:523–32.
602 https://doi.org/10.1016/j.fuel.2017.10.045.
603 [33] Kirtania K, Axelsson J, Matsakas L, Christakopoulos P, Umeki K, Furusjö E. Kinetic
604 study of catalytic gasification of wood char impregnated with different alkali salts.
605 Energy 2017;118:1055–65. https://doi.org/10.1016/j.energy.2016.10.134.
606 [34] Meijer R, Kapteijn F, Moulijn JA. Kinetics of the alkali-carbonate catalysed gasification
607 of carbon: 3. H2O gasification. Fuel 1994;73:723–30. https://doi.org/10.1016/0016-
608 2361(94)90015-9.
609 [35] Mudge LK, Sealock LJ, Weber SL. Catalyzed steam gasification of biomass. J Anal
610 Appl Pyrolysis 1979;1:165–75. https://doi.org/10.1016/0165-2370(79)80013-3.
611 [36] Perander M, DeMartini N, Brink A, Kramb J, Karlström O, Hemming J, et al. Catalytic
612 effect of Ca and K on CO2 gasification of spruce wood char. Fuel 2015;150:464–72.
613 https://doi.org/10.1016/j.fuel.2015.02.062.
614 [37] Elliott DC, Hallen RT, Sealock LJ. Alkali catalysis in biomass gasification. J Anal Appl
615 Pyrolysis 1984;6:299–316. https://doi.org/10.1016/0165-2370(84)80024-8.
616 [38] European Standards. Solid biofuels - Determination of ash content (EN 14775). 2009.

[39] International Organization for Standardization. Solid biofuels - Determination of major elements - Al, Ca, Fe, Mg, P, K, Si, Na and Ti (ISO 16967:2015). 2015.

[40] Vassilev SV, Baxter D, Andersen LK, Vassileva CG, Morgan TJ. An overview of the organic and inorganic phase composition of biomass. Fuel 2012;94:1–33. https://doi.org/10.1016/j.fuel.2011.09.030.

[41] Barrio M, Gøbel B, Rimes H, Henriksen U, Hustad JE, Sørensen LH. Steam Gasification of Wood Char and the Effect of Hydrogen Inhibition on the Chemical Kinetics. In: Bridgwater AV, editor. Prog. Thermochem. Biomass Convers., John Wiley & Sons, Ltd; 2001, p. 32–46. https://doi.org/10.1002/9780470694954.ch2.

[42] Bale CW, Chartrand P, Degterov SA, Eriksson G, Hack K, Ben Mahfoud R, et al. FactSage thermochemical software and databases. Calphad 2002;26:189–228. https://doi.org/10.1016/S0364-5916(02)00035-4.

[43] Hack K, Jantzen T, Müller M, Yazhenskikh E, Wu G. A novel thermodynamic database for slag systems and refractory materials. In Proceedings of the 5th International Congress on the Science and Technology of Steelmaking 2012.

[44] Defoort F, Froment K. Thermodynamical analysis of the fission product release in the ORNL VI-3 and VI-5 tests (in French). Grenoble: 1998.

[45] Anca-Couce A. Reaction mechanisms and multi-scale modelling of lignocellulosic biomass pyrolysis. Prog Energy Combust Sci 2016;53:41–79. https://doi.org/10.1016/j.pecs.2015.10.002.

[46] Dahou T. Contribution to the understanding of the role of inorganic elements in biomass steam gasification. PhD thesis. Université Grenoble Alpes (ComUE), 2019.

[47] Arvelakis S, Jensen PA, Dam-Johansen K. Simultaneous Thermal Analysis (STA) on Ash from High-Alkali Biomass. Energy Fuels 2004;18:1066–76. https://doi.org/10.1021/ef034065+.

[48] Knudsen JN, Jensen PA, Dam-Johansen K. Transformation and Release to the Gas Phase of Cl, K, and S during Combustion of Annual Biomass. Energy Fuels 2004;18:1385–99. https://doi.org/10.1021/ef049944q.

[49] Zhao H, Xu W, Song Q, Zhuo J, Yao Q. Effect of Steam and SiO2 on the Release and Transformation of K2CO3 and KCl during Biomass Thermal Conversion. Energy Fuels 2018. https://doi.org/10.1021/acs.energyfuels.8b02269.

[50] Sergeev D, Yazhenskikh E, Kobertz D, Müller M. Vaporization behavior of Na2CO3 and K2CO3. Calphad 2019;65:42–9. https://doi.org/10.1016/j.calphad.2019.02.004.

[51] Wood BJ, Sancier KM. The Mechanism of the Catalytic Gasification of Coal Char: A Critical Review. Catal Rev 1984;26:233–79. https://doi.org/10.1080/01614948408078065.

[52] de Wild P. Biomass pyrolysis for chemicals. University of Groningen, 2011.

[53] Di Blasi C, Galgano A, Branca C. Effects of Potassium Hydroxide Impregnation on Wood Pyrolysis. Energy Fuels 2009;23:1045–54. https://doi.org/10.1021/ef800827q.

[54] Zaror CA, Hutchings IS, Pyle DL, Stiles HN, Kandiyoti R. Secondary char formation in the catalytic pyrolysis of biomass. Fuel 1985;64:990–4. https://doi.org/10.1016/0016-2361(85)90156-5.

[55] Zhao D, Dai Y, Chen K, Sun Y, Yang F, Chen K. Effect of potassium inorganic and organic salts on the pyrolysis kinetics of cigarette paper. J Anal Appl Pyrolysis 2013;102:114–23. https://doi.org/10.1016/j.jaap.2013.03.007.

[56] Björkman E, Strömberg B. Release of Chlorine from Biomass at Pyrolysis and Gasification Conditions. Energy Fuels 1997;11:1026–32. https://doi.org/10.1021/ef970031o.

[57] Bridgwater AV. Pyrolysis of Biomass. In: Van Swaaij WPM, Kersten SRA, Palz W, editors. Biomass Power World Transform. Eff. Use, Singapore: Pan Stanford Publishing; 2015, p. 473–513.

[58] Marsh H, Rodríguez-Reinoso F. CHAPTER 6 - Activation Processes (Chemical). In: Marsh H, Rodríguez-Reinoso F, editors. Act. Carbon, Oxford: Elsevier Science Ltd; 2006, p. 322–65. https://doi.org/10.1016/B978-008044463-5/50020-0.

671 [59] Gupta A, Thengane SK, Mahajani S. CO2 gasification of char from lignocellulosic
672 garden waste: Experimental and kinetic study. Bioresour Technol 2018;263:180–91.
673 https://doi.org/10.1016/j.biortech.2018.04.097.
674 [60] Sueyasu T, Oike T, Mori A, Kudo S, Norinaga K, Hayashi J. Simultaneous Steam
675 Reforming of Tar and Steam Gasification of Char from the Pyrolysis of Potassium-
676 Loaded Woody Biomass. Energy Fuels 2012;26:199–208.
677 https://doi.org/10.1021/ef201166a.
678